



1 **Stem and soil nitrous oxide fluxes from rainforest and cacao**
2 **agroforest on highly weathered soils in the Congo Basin**

3 Najeeb A. Iddris¹, Marife D. Corre¹, Martin Yemefack^{2,3}, Oliver van Straaten^{1,4}, Edzo

4 Veldkamp¹

5 ¹Soil Science of Tropical and Subtropical Ecosystems, University of Goettingen, Goettingen,

6 37077, Germany

7 ²International Institute of Tropical Agriculture, Yaoundé, Cameroon

8 ³ Now at: Sustainable Tropical Solutions (STS), Yaoundé, Cameroon

9 ⁴ Now at: Northwest German Forest Research Institute, Goettingen, 37079, Germany

10 *Correspondence to:* N. A. Iddris (nidris@gwdg.de)



11 **Abstract.** Although tree stems act as conduits for greenhouse gases (GHG) produced in the soil,
12 the magnitudes of tree contributions to total (soil + stem) nitrous oxide (N₂O) emissions from
13 tropical rainforests on heavily weathered soils remain unknown. Moreover, soil GHG fluxes are
14 largely understudied in African rainforests, and the effects of land-use change on these gases are
15 identified as an important research gap in the global GHG budget. In this study, we quantified
16 the changes in stem and soil N₂O fluxes with forest conversion to cacao agroforestry. Stem and
17 soil N₂O fluxes were measured monthly for a year (2017–2018) in four replicate plots per land
18 use at three sites across central and southern Cameroon. Tree stems consistently emitted N₂O
19 throughout the measurement period, and were positively correlated with soil N₂O fluxes. ¹⁵N-
20 isotope tracing from soil mineral N to stem-emitted ¹⁵N₂O as well as correlations between
21 temporal patterns of stem N₂O emissions, soil-air N₂O concentration, soil N₂O emissions, and
22 vapor pressure deficit suggest that N₂O emitted by the stems originated predominantly from N₂O
23 produced in the soil. Forest conversion to extensively managed, mature (> 20 years old) cacao
24 agroforestry had no effect on stem and soil N₂O fluxes. The annual total N₂O emissions were
25 $1.55 \pm 0.20 \text{ kg N ha}^{-1} \text{ yr}^{-1}$ from the forest and $1.15 \pm 0.10 \text{ kg N ha}^{-1} \text{ yr}^{-1}$ from cacao agroforestry,
26 with tree N₂O emissions contributing 11 to 38 % for forests and 8 to 15 % for cacao agroforestry.
27 These substantial contributions of tree stems to total N₂O emissions highlight the importance of
28 including tree-mediated fluxes in ecosystem GHG budgets. Taking into account that our study
29 sites' biophysical characteristics represented two-thirds of the humid rainforests in the Congo
30 Basin, we estimated a total N₂O source strength for this region of $0.18 \pm 0.05 \text{ Tg N}_2\text{O yr}^{-1}$.

31 **1. Introduction**

32 The trace gas nitrous oxide (N₂O) has become the main stratospheric ozone depleting substance
33 produced by human activities (Ravishankara et al., 2009), and is after carbon dioxide and methane
34 (CH₄) the most important anthropogenic greenhouse gas (GHG) (Denman et al., 2007). Humid



35 tropical soils are considered one of the most important global N₂O sources (Denman et al., 2007;
36 Werner et al., 2007a), with tropical rainforests alone estimated to contribute between 0.9 to 4.5
37 Tg N₂O-N yr⁻¹ to the global N₂O source of about 16 Tg N₂O-N yr⁻¹ (Bouwman et al., 1995;
38 Breuer et al., 2000; Werner et al., 2007a). However, ground-based, bottom-up N₂O emission
39 estimates appear to be in stark contrast to the high emissions estimated from top-down approaches
40 such as modelling and global N₂O atmospheric inversions (Huang et al., 2008; Thompson et al.,
41 2014). Nevertheless, there exists considerable uncertainty in both approaches (Davidson and
42 Kanter, 2014), especially for the tropics (Valentini et al., 2014). Recent studies suggest two
43 possible reasons for large uncertainties in bottom-up approaches: “missing” emission pathways
44 such as trees (Welch et al., 2019), and a strong geographic bias of measured N₂O fluxes from
45 tropical forests.

46 Most of the studies on soil N₂O fluxes from tropical ecosystems were conducted in South
47 and Central America (Davidson and Verchot, 2000; Matson et al., 2017; Neill et al., 2005; Wolf
48 et al., 2011), tropical Asia (Hassler et al., 2017; Purbopuspito et al., 2006; Veldkamp et al., 2008;
49 Verchot et al., 2006; Werner et al., 2006) and Australia (Breuer et al., 2000; Kiese et al., 2003).
50 Africa remains the continent with the least published field studies on soil N₂O fluxes from the
51 tropical forest biome. After the pioneering work by Serca et al. (1994), very few field studies
52 have been conducted, most of which were either not replicated with independent plots or only
53 with short measurement campaigns (Castaldi et al., 2013; Gütlein et al., 2018; Wanyama et al.,
54 2018; Werner et al., 2007b). The remaining studies were based on laboratory incubations, which
55 cannot be translated to actual field conditions. Consequently, field-based studies with sufficient
56 spatial and temporal coverage are critical for improving the highly uncertain N₂O sink and source
57 estimates for Africa (Kim et al., 2016b; Valentini et al., 2014).

58 The Congo Basin is the second largest intact tropical forest in the world and constitutes
59 one of the most important carbon (C) and biodiversity reservoirs globally. Behind the DR Congo,



60 Cameroon is the second highest deforested country in the Congo Basin with about 75 % of its
61 forest being subject to pressure from other land uses including agroforestry (Dkamela, 2010).
62 Conversion of forests to traditional cacao agroforestry (CAF) systems have well been
63 documented in Cameroon (Saj et al., 2013; Sonwa et al., 2007; Zapfack et al., 2002). Presently,
64 an estimated 400,000 hectares is under CAF on small family farms of approximately one to three
65 hectares (Kotto et al., 2002; Saj et al., 2013). These CAF systems are commonly established under
66 the shade of the forests' remnant trees, and are characterised by absence of fertilizer inputs and
67 low yields of up to 1 t cacao beans ha⁻¹ (Saj et al., 2013).

68 Changes in land use have been found to affect soil N₂O emissions due to changes in soil
69 N availability (Corre et al., 2006), vegetation (Veldkamp et al., 2008) and management practices
70 such as N fertilization (Hassler et al., 2017). In particular, unfertilized agroforestry and
71 agricultural systems have been found to have comparable N₂O fluxes as those from the reference
72 forests (Hassler et al., 2017), whereas N-fertilized systems tend to have higher N₂O fluxes than
73 the previous forest due to elevated soil mineral N following fertilization (Verchot et al., 2006).
74 This is in line with postulations of the conceptual hole-in-the-pipe (HIP) model, which suggest
75 that the magnitude of N₂O emissions from the soil are largely controlled first by soil N availability
76 and second by soil water content (Davidson et al., 2000). A systematic comparison between a
77 reference land use and a converted system for quantifying land-use change effects on GHG fluxes
78 is virtually lacking for the Congo Basin, and thus an important knowledge gap in the GHG budget
79 of Africa (Valentini et al., 2014).

80 Tree stems have been found to act as conduits for soil N₂O in wetlands, mangroves and
81 well-drained forests (Kreuzwieser et al., 2003; Rusch and Rennenberg, 1998; Welch et al., 2019),
82 facilitating the transport from the soil, where N₂O are produced or consumed by microbial
83 nitrification and denitrification processes, to the atmosphere. Findings of strong declines in N₂O
84 emissions with increasing stem height (Barba et al., 2019; Díaz-Pinés et al., 2016; Rusch and



85 Rennenberg, 1998; Wen et al., 2017) suggest that N₂O is mainly emitted through the stems and
86 less likely through the leaves. Trees adapted to wetlands and mangroves have aerenchyma
87 systems through which N₂O can be transported from the soil into the tree by both gas diffusion
88 and transpiration stream, with exchange to the atmosphere predominantly through the stem
89 lenticels (Rusch and Rennenberg, 1998; Wen et al., 2017). However, for trees on well-drained
90 soils, a different transport mechanism appears to be dominant: transpiration drives the xylem sap
91 flow in which dissolved N₂O is transported from the soil to the tree and emitted to the atmosphere
92 through the stem surface and stomata (Machacova et al., 2013; Wen et al., 2017). Recent evidence
93 shows that trees can also act as N₂O sinks (Barba et al., 2019; Machacova et al., 2017),
94 highlighting the need for further research of the stem N₂O flux magnitudes and their mechanisms.

95 The most important soil parameters found to influence tree-stem N₂O fluxes include soil
96 water content (Machacova et al., 2016; Rusch and Rennenberg, 1998), soil N₂O fluxes (Díaz-
97 Pinés et al., 2016; Wen et al., 2017), soil temperature (Machacova et al., 2013) and soil-air N₂O
98 concentration within the rooting zone (Machacova et al., 2013; Wen et al., 2017). These studies
99 also reported environmental parameters, such as air temperature and vapour pressure deficit, to
100 drive stem N₂O fluxes due to their influence on transpiration (O'Brien et al., 2004). For temperate
101 forests on a well-drained soil, annual stem N₂O fluxes have been found to contribute up to 10 %
102 of the ecosystem N₂O emissions (Wen et al., 2017). However, until now, there is no ground-
103 based spatial extrapolation of the contribution of stem N₂O emissions from tropical forests on
104 well-drained soils. Hence, there is a need for concurrent quantifications of the contributions of
105 stem and soil N₂O fluxes so as to provide insights on the source strengths of N₂O emissions from
106 tropical African land uses and to improve estimates of N₂O emissions from the region.

107 Our present study addresses these knowledge gaps by providing year-round
108 measurements of stem and soil N₂O fluxes from forests and converted CAF systems with spatially
109 replicated plots in the Congo Basin as well as stem N₂O fluxes of 23 tree species that have not



110 been measured before. Our findings contribute to the much-needed improvement of GHG budget
111 from this region. Our study aimed to (i) assess whether trees in tropical rainforests and CAF are
112 important conduits of N₂O, (ii) quantify changes in soil-atmosphere N₂O fluxes with forest
113 conversion to CAF, and (iii) determine the temporal and spatial controls of stem and soil N₂O
114 fluxes. We hypothesized that (i) stem and soil N₂O fluxes from these extensively managed CAF
115 systems (unfertilized and manual harvest) will be comparable to the natural forests, and (ii) the
116 seasonal pattern of stem emissions will parallel that of soil N₂O emissions and both will have
117 similar soil and climatic controlling factors.

118 **2. Materials and methods**

119 **2.1 Study area and experimental design**

120 Our study was conducted at three study sites located in southern and central Cameroon, where
121 natural forests are predominantly converted to CAF (Sonwa et al., 2007). Sites in the southern
122 region were located around the villages of Aloum (2.813° N, 10.719° E; 651 m above sea level,
123 asl) and Biba Yezoum (3.158° N, 12.292° E; 674 m asl), and the third site was located around the
124 village of Tomba (3.931° N, 12.430° E; 752 m asl) in the central region (Fig. B1). The mean
125 annual air temperature across the three sites is 23.5 °C (Climate-Data.org, 2019), and the soil
126 temperature ranged from 21.6–24.4 °C during our measurement period from May 2017 to April
127 2018. The study sites span an annual precipitation from 1576 mm yr⁻¹ in the central to 2064 mm
128 yr⁻¹ in the south of Cameroon (Table A1; Climate-Data.org, 2019). Precipitation occurs in a
129 bimodal pattern, with two dry seasons (< 120 mm monthly rainfall) occurring from July to August
130 and December to February. All sites are situated on heavily weathered soils classified as
131 Ferralsols (FAO classification; IUSS Working Group WRB, 2015). Geologically, Tomba and
132 Biba Yezoum are underlain by middle to superior Precambrian basement rocks (metamorphic
133 schists, phyllites and quartzites), whereas Aloum site is situated on inferior Precambrian
134 basement rocks (inferior gneiss and undifferentiated gneiss) (Gwanfogne et al., 1983).



135 At each of the three sites, we studied two land–use systems: the reference forest and the
136 converted CAF system. Additional information on vegetation and site characteristics are reported
137 in Table A1. These CAF sites were established right after clearing the natural forests, where
138 remnant forest trees were retained by farmers to provide shade for understorey cacao trees
139 (*Theobroma cacao*). Cacao planting and localised weeding were all done manually using hand
140 tools. Interviews of farm owners indicated that there had been no mineral fertilization in any of
141 the CAF sites. The ages of the CAF since conversion varied between 22 and ~ 45 years.

142 We selected four replicate plots (50 m x 50 m each with a minimum distance of 100 m
143 between plots) per land-use type within each site (Fig. B1), totalling to 24 plots that were all
144 located on relatively flat topography. Within each plot, all stems including cacao trees with a
145 diameter at breast height (DBH) ≥ 10 cm were identified and measured for DBH and height. We
146 conducted N₂O flux measurements, soil and meteorological parameters in the inner 40 m × 40 m
147 area within each plot to minimize edge effects. To check that soil conditions were comparable
148 between the reference forests and converted CAF, we compared a land-use-independent soil
149 characteristic, i.e. clay content at 30–50 cm depth, between these land uses at each site. Since we
150 did not find significant differences in clay contents between the forest and CAF at each site (Table
151 1), we inferred that land-use types within each site had comparable initial soil characteristics prior
152 to conversion and any differences in N₂O fluxes and soil controlling factors can be attributed to
153 land-use conversion.

154 For measurements of stem N₂O fluxes, we selected six cacao trees per replicate plot in the
155 CAF, and six trees representing the most dominant species within each replicate plot in the forest,
156 based on their importance value index (IVI) (Table A1). The species IVI is a summation of the
157 relative density, relative frequency and relative dominance of the tree species (Curtis and
158 McIntosh, 1951). For a given species, the relative density refers to its total number of individuals
159 in the four forest plots at each site; the relative frequency refers to its occurrence among the four



160 forest plots; and the relative dominance refers to its total basal area in the four forest plots, all
161 expressed as percentages of all species. These 24 trees measured at each site (6 trees x 4 forest
162 plots) included nine species in Aloum site, seven species in Biba Yezoum site, and 10 species in
163 Tomba site (species are specified in Fig. 1). The trees were measured for stem N₂O fluxes at 1.3
164 m height above the ground at monthly interval from May 2017 to April 2018. Furthermore, we
165 assessed the influence of tree height on stem N₂O fluxes by conducting additional measurements
166 on 16 individual trees per land use in May 2018; these trees were included in the monthly
167 measurements but were additionally measured at three stem heights (1.3 m, 2.6 m and 3.9 m from
168 the ground) per tree in the forest, and at two heights (1.3 m and 2.6 m) per tree in the CAF due to
169 the limited height of the cacao trees.

170 For soil N₂O flux measurements, we installed four permanent chamber bases per replicate
171 plot which were randomly distributed within the inner 40 m × 40 m area. We conducted monthly
172 measurements of soil N₂O fluxes from May 2017 to April 2018 as well as meteorological and
173 soil variables known to control N₂O emission (see below).

174 **2.2 Measurement of stem and soil N₂O fluxes**

175 We measured in situ stem N₂O fluxes using stem chambers made from transparent
176 polyethylene-terephthalate foil, as described by Wen et al. (2017). One month prior to
177 measurement, we applied acetic acid-free silicone sealant strips (Otto Seal ® S110, Hermann
178 Otto GmbH, Fridolfing, Germany) of about 1 cm wide at 20 cm apart around the surface of the
179 tree stems (between 1.2 m and 1.4 m heights from the ground) that stayed permanently to ensure
180 that all the stem chambers had air-tight seals (Fig. B2). As many of the measured trees have
181 buttresses (rendering stem chambers impossible to attach at low stem height, e.g. Fig. B2), we
182 chose the measurements at an average of 1.3 m height (or between 1.2–1.4 m), congruent to the
183 standard measurement of DBH. Since chamber installation is quick, chambers were newly
184 installed on each sampling date, using the silicone sealant strips as a mark to ensure that the same



185 0.2 m length stem section was measured. We wrapped a piece of foil (cut approximately 50 cm
186 longer than the measured stem circumference and fitted with a Luer lock sampling port) around
187 each stem. Using a gas-powered heat gun, we “shrank” the top and bottom part of the foil to fit
188 closely onto the silicone strips, leaving 0.2 m length between the top and bottom silicone strips,
189 which served as the chamber for collecting gas samples (Fig. B2). We then wrapped strips of
190 polyethylene foam around the edges of the foil and adjusted the foam tightly using lashing straps
191 equipped with ratchet tensioners (two straps at the top and two at the bottom). The lashing straps
192 adjusted the flexible foam and the foil (on top of the silicone strips) to any irregularities on the
193 bark and ensured an airtight fitting. After installation, we completely evacuated the air inside the
194 stem chamber using a syringe fitted with a Luer lock one-way check valve. Afterwards, we used
195 a manual hand pump to refill the stem chamber with a known volume of ambient outside air for
196 correct calculation of stem N₂O flux. A 25 mL air sample was taken with syringe through the
197 Luer lock sampling port immediately after refilling the stem chamber with ambient air, and then
198 again after 20, 40 and 60 min. Each air sample was immediately stored in pre-evacuated 12 mL
199 Labco exetainers with rubber septa (Labco Limited, Lampeter, UK), maintaining an overpressure.

200 In May 2018, we conducted a ¹⁵N tracing experiment at the Tomba site as a follow-on
201 study to elucidate the source of stem N₂O emissions. The tracing was conducted in three replicate
202 plots per land use, where one tree was selected in each plot. Around each selected tree, 290 mg
203 ¹⁵N (in the form of (¹⁵NH₄)₂SO₄ with 98 % ¹⁵N) dissolved in 8 L distilled water was applied
204 evenly onto the soil surface of 0.8 m² around the tree using a watering can (equivalent to 10 mm
205 of rain). The water-filled pore space (WFPS) in the top 5 cm depth was 49 ± 1 % and 52 ± 2 %
206 for the forest and CAF, respectively, which were within the range of monthly average WFPS of
207 these plots (Fig. 2i). Based on the monthly average soil mineral N concentrations in these plots,
208 the applied ¹⁵N was only 20 % of the extant mineral N in the top 10 cm soil (resulting to a starting
209 enrichment of 17 % ¹⁵N), such that we only minimally changed the substrate which could



210 influence N₂O flux, similar to that described by Corre, Sueta, & Veldkamp, (2014). Stem and soil
211 ¹⁵N₂O fluxes were measured one day, seven days and 14 days following ¹⁵N application, and on
212 each sampling day gas samples were taken at 0, 30, and 60 min after chamber closure. The gas
213 samples were stored in new pre-evacuated glass containers (100 mL) with rubber septa and
214 transported to the University of Goettingen, Germany for analysis. We also stored ¹⁵N₂O
215 standards in similar 100 mL glass containers, which were brought to Cameroon and back to
216 Germany, to have the same storage duration as the gas samples in order to check for leakage; we
217 found no difference in ¹⁵N₂O with the original standard at our laboratory.

218 We measured soil N₂O fluxes using vented, static chambers made from polyvinyl chloride
219 that were permanently inserted ~ 0.02 m into the soil at least one month prior to the start of
220 measurements, as described in our earlier studies (e.g., Corre et al., 2014; Koehler et al., 2009;
221 Müller et al., 2015). On each sampling day, we covered the chamber bases with vented, static
222 polyethylene hoods (0.04 m² in area and ~ 11 L total volume) equipped with Luer lock sampling
223 ports. Soil N₂O fluxes were then determined by taking four gas samples (25 mL each) at 2, 12,
224 22 and 32 min after chamber closure. The samples were taken with a syringe and immediately
225 injected into pre-evacuated 12 mL exetainers as described above.

226 Concurrent to the stem and soil N₂O flux measurements, we sampled soil-air N₂O
227 concentrations at 50 cm depth from permanently installed stainless steel probes (1 mm internal
228 diameter) located at ~ 1 m from the measured trees. The stainless steel probes were installed one
229 month prior to the start of measurements. Luer locks were attached to the probes, and on each
230 sampling day the probes were first cleared of any previous accumulation of N₂O concentration
231 by removing 5 mL air volume using a syringe and discarding it. We then took 25 mL gas samples
232 and stored them in pre-evacuated 12 mL exetainers as described above.



233 2.3 N₂O analysis and flux rate calculation

234 The N₂O concentrations in the gas samples were analysed using a gas chromatograph equipped
235 with an electron capture detector, a make-up gas of 5 % CO₂ – 95 % N₂ (SRI 8610C, SRI
236 Instruments Europe GmbH, Bad Honnef, Germany), and an autosampler (AS-210, SRI
237 Instruments). ¹⁵N₂O was analysed on an isotope ratio mass spectrometer (IRMS) (Finnigan
238 Deltaplus XP, Thermo Electron Corporation, Bremen, Germany). We calculated N₂O fluxes from
239 the linear change in concentrations over time of chamber closure, and adjusted the fluxes with air
240 temperature and atmospheric pressure, measured at each replicate plot on each sampling day. We
241 included zero and negative fluxes in our data analysis.

242 We up-scaled the measured stem N₂O fluxes (considering trees ≥ 10 cm DBH) to annual
243 values on a ground area in the following steps: (1) the relationship between stem N₂O fluxes and
244 stem heights was modelled from the 16 individual trees per land use (see above) that were
245 measured at multiple heights, from which we observed decreases in stem N₂O fluxes with
246 increasing stem heights. A linear function was statistically the best fit characterizing these
247 decreases in stem N₂O fluxes with height. (2) Using this linear function and considering the stem
248 surface area as a frustum with 20 cm increment, the tree-level N₂O fluxes on each sampling day
249 was calculated for the regularly measured six trees per plot. (3) The annual tree-level N₂O fluxes
250 from these regularly measured six trees per plot were calculated using a trapezoidal interpolation
251 between the tree-level N₂O fluxes (step 2) and measurement day intervals from May 2017 to
252 April 2018. (4) The annual tree-level N₂O fluxes were then extrapolated on a ground–area basis
253 for each replicate plot as follows (Eq. 1):

$$254 \quad \text{Annual stem N}_2\text{O flux (kg N}_2\text{O-N ha}^{-1} \text{ yr}^{-1}) = \frac{\left\{ \sum \left[\left(\frac{X_{1-24} / \text{DBH}_{1-24}}{24} \right) * \text{DBH}_n \right] \right\}}{A} \quad (1)$$

255 where X_{1-24} and DBH_{1-24} are the corresponding annual tree-level N₂O flux (kg N₂O-N yr⁻¹ of
256 each tree; step 3) and DBH (cm) of each of the 24 measured trees (6 trees x 4 plots) per land use



257 at each site, DBH_n is the individual tree DBH (cm) measured for all trees (with ≥ 10 cm DBH)
258 present within the inner $40 \text{ m} \times 40 \text{ m}$ area of each plot (Table A1), Σ is the sum of the annual
259 N_2O fluxes of all trees within each plot ($\text{kg N}_2\text{O-N yr}^{-1}$) and A is the plot area (0.16 ha).

260 For step 4 of the CAF plots, the annual stem N_2O flux was the sum of the cacao and shade
261 trees (Table A1); as these shade trees were remnants of the original forest, we used the average
262 annual tree-level N_2O flux of the measured trees in the corresponding paired forest plots
263 multiplied by the actual DBH of the shade trees in the CAF plots. This spatial extrapolation based
264 on trees' DBH of each plot was also supported by the fact that there were no significant
265 differences in stem N_2O fluxes among tree species (Fig. 1).

266 Annual soil N_2O fluxes from each plot were calculated using the trapezoidal rule to
267 interpolate the measured fluxes from May 2017 to Apr. 2018, as employed in our earlier studies
268 (e.g., Koehler et al., 2009; Veldkamp et al., 2013). Finally, the annual N_2O fluxes from each
269 replicate plot were represented by the sum of the stem and soil N_2O fluxes.

270 **2.4 Soil and meteorological variables**

271 We measured soil temperature, WFPS, and extractable mineral N in the top 5 cm depth concurrent
272 to stem and soil N_2O flux measurements on each sampling day. The soil temperature was
273 measured ~ 1 m away from the soil chambers using a digital thermometer (GTH 175, Greisinger
274 Electronic GmbH, Regenstauf, Germany). We determined soil WFPS and extractable mineral N
275 by pooling soil samples from four sampling locations within 1 m from each soil chamber in each
276 replicate plot. Gravimetric moisture content was determined by oven-drying the soils at 105°C
277 for 24 h and WFPS was calculated using a particle density of 2.65 g cm^{-3} for mineral soil and our
278 measured soil bulk density (Table 1). Soil mineral N (NO_3^- and NH_4^+) was extracted in the field
279 by putting a subsample of soil into a pre-weighed bottle containing 150 mL 0.5 M K_2SO_4 . The
280 bottles were weighed and then shaken for 1 h, and the solution was filtered through pre-washed
281 (with 0.5 M K_2SO_4) filter papers. The extracts were immediately frozen and later transported to



282 the University of Goettingen, where NH_4^+ and NO_3^- concentrations were analysed using
283 continuous flow injection colorimetry (SEAL Analytical AA3, SEAL Analytical GmbH,
284 Norderstedt, Germany) (described in details by Hassler et al., 2015). The dry mass of soil
285 extracted for mineral N was calculated using the measured gravimetric moisture content.

286 During each measurement day, we set up a portable weather station in each site to record
287 relative humidity and air temperature over the course of each sampling day at 15 min interval.
288 We calculated vapour pressure deficit (VPD) as the difference between saturation vapour
289 pressure (based on its established equation with air temperature) and actual vapour pressure
290 (using saturation vapour pressure and relative humidity; Allen et al., 1998).

291 Soil biochemical characteristics were measured in April 2017 at all 24 plots. We collected
292 soil samples from the top 50 cm depth, where changes in soil biochemical characteristics resulting
293 from land-use changes have been shown to occur (van Straaten et al., 2015; Tchifofo Lontsi et al.,
294 2019). In each plot, we collected ten soil samples from the top 0–10 cm, and five soil samples
295 each from 10–30 and 30–50 cm depths; in total, we collected 480 soil samples from the 24 plots.
296 The soil samples were air dried, sieved (2 mm) and transported to the University of Goettingen,
297 where they were dried again at 40 °C before analysis. Soil pH was analysed from 1:4 soil to
298 distilled water ratio. Soil texture for each plot was determined using the pipette method after iron
299 oxide and organic matter removal (Kroetsch and Wang, 2008). Effective cation exchange
300 capacity (ECEC) and exchangeable cation concentrations (Ca, Mg, K, Na, Al, Fe, Mn) were
301 determined by percolating the soil samples with unbuffered 1 M NH_4Cl , and the extracts analysed
302 using inductively coupled plasma-atomic emission spectrometer (ICP-AES; iCAP 6300 Duo
303 VIEW ICP Spectrometer, Thermo Fischer Scientific GmbH, Dreieich, Germany). Soil
304 subsamples were ground and analysed for total organic C and N using a CN analyser (vario EL
305 cube; Elementar Analysis Systems GmbH, Hanau, Germany), and the soil ^{15}N natural abundance
306 signatures were determined using IRMS (Delta Plus; Finnigan MAT, Bremen, Germany). Soil



307 organic carbon (SOC) and total N stocks were calculated for the top 50 cm in both land uses. We
308 used the bulk density of the reference forest for calculating the SOC and total N stocks of the
309 converted CAF in order to avoid overestimations of element stocks resulting from increases in
310 soil bulk densities following land-use conversion (van Straaten et al., 2015; Veldkamp, 1994).

311 To evaluate the representativeness of our study area with the rest of the Congo Basin
312 rainforest, we estimated the proportion of the Congo rainforest area which have similar
313 biophysical conditions (elevation, precipitation ranges and soil type) as our study sites (Table
314 A1). Using the FAO's Global Ecological Zone map for the humid tropics, we identified the areal
315 coverage of (i) Ferralsols (FAO Harmonized World Soil Database; FAO/IIASA/ISRIC/ISS-
316 CAS/JRC, 2012) with (ii) elevation ≤ 1000 m asl (SRTM digital elevation model; Jarvis, Reuter,
317 Nelson, & Guevara, 2008) and (iii) precipitation range between 1,500 and 2,100 mm yr⁻¹
318 (WorldClim dataset; Hijmans et al., 2005) within the six Congo rainforest countries (Fig. B3).
319 This analysis was conducted using QGIS version 3.6.3.

320 2.5 Statistical analyses

321 Statistical comparisons between land uses or among sites for stem and soil N₂O fluxes were
322 performed on the monthly measurements and not on the annual values as the latter are trapezoidal
323 interpolations. As the six trees and four chambers per plot were considered subsamples
324 representing each replicate plot, we conducted the statistical analysis using the means of the six
325 trees and of the four chambers on each sampling day for each replicate plot (congruent to our
326 previous studies, e.g., Hassler et al., 2017; Matson et al., 2017). We tested each parameter for
327 normal distribution (Shapiro–Wilk's test) and homogeneity of variance (Levene's test), and
328 applied a logarithmic or square root transformation when these assumptions were not met. For
329 the repeatedly measured parameters, i.e. stem and soil N₂O fluxes and the accompanying soil
330 variables (temperature, WFPS, NH₄⁺ and NO₃⁻ concentrations), differences between land-use
331 types for each site or differences among sites for each land-use type were tested using linear



332 mixed effect (LME) models with land use or site as fixed effect and replicate plots and sampling
333 days as random effects (Crawley, 2009). We assessed significant differences between land uses
334 or sites using analysis of variance (ANOVA) with Tukey's HSD test.

335 We also analysed if there were differences in stem N₂O fluxes among tree species across
336 four forest plots at each site as well as across the three sites. Similar LME analysis was carried
337 out with tree species as fixed effect, and the random effects were trees belonging to each species
338 and sampling days; only for this test, we used individual trees as random effect because most of
339 the tree species (selected based on their IVI; see Sect. 2.1.) were not present in all plots, which is
340 typical in species-diverse tropical forest. For soil biochemical characteristics that were measured
341 once (Table1), one-way ANOVA followed by a Tukeys's HSD test was used to assess the
342 differences between land uses or sites for the variables with normal distribution and homogenous
343 variance; if otherwise, we applied Kruskal-Wallis ANOVA with multiple comparison extension
344 test.

345 To determine the temporal controls of soil and meteorological variables (temperature,
346 WFPS, NH₄⁺ and NO₃⁻ concentrations, soil-air N₂O concentration, VPD) on stem and soil N₂O
347 fluxes, we conducted Spearman's Rank correlation tests using the means of the four replicate
348 plots for each land use on each sampling day. For each land use, the correlation tests were
349 conducted across sites and sampling days ($n = 33$, from 3 sites \times 11 monthly measurements). To
350 determine the spatial controls of soil biochemical characteristics (which were measured once,
351 Table 1) on stem and soil N₂O fluxes, we used the plots' annual N₂O emissions and tested with
352 Spearman's Rank correlation across land uses and sites ($n = 24$, from 3 sites \times 2 land uses \times 4
353 replicate plots). The statistical significance for all the tests were set at $P \leq 0.05$. All statistical
354 analyses were conducted using the open source software R 3.5.2 (R Core Team, 2018).



355 **3 Results**

356 **3.1 Stem N₂O emissions**

357 Stem N₂O emissions neither differed between forest and CAF at each site ($P = 0.15$ – 0.76 ; Table
358 2) nor among the three sites for each land use ($P = 0.16$ – 0.78 ; Table 2). There were also no
359 differences in stem N₂O emissions among tree species in forest plots at each site as well as across
360 the three sites ($P = 0.06$ – 0.39 ; Fig. 1). For the forests, stem N₂O emissions exhibited seasonal
361 pattern with larger fluxes in the wet season than in the dry season at all sites (all $P < 0.01$; Table
362 A2; Fig. 2a, b, c). However, for the CAF, we observed seasonal differences only at Aloum site
363 ($P < 0.01$; Table A3; Fig. 2a). Contributions of annual stem N₂O emissions reached up to one-
364 third of the total (stem + soil) N₂O emissions from the forests (Table 2).

365 From the ¹⁵N-tracing experiment, stem ¹⁵N-N₂O emissions mirrored soil ¹⁵N-N₂O
366 emissions from both land uses (Fig. 3). One day after ¹⁵N addition to the soil, substantial ¹⁵N-
367 N₂O were emitted from the stem as well as from the soil. This diminished within two weeks as
368 the added ¹⁵N recycled within the soil N cycling processes, diluting the ¹⁵N signatures;
369 nevertheless, the ¹⁵N signatures of stem- and soil-emitted N₂O remained elevated above the
370 natural abundance level (Fig. 3).

371 Across the study period, stem N₂O emissions from the forests were positively correlated
372 with air temperature, soil-air N₂O concentrations and VPD (Table 3) and negatively correlated
373 with WFPS and NH₄⁺ contents (Table 3). The negative correlation of stem N₂O emissions with
374 WFPS was possibly spurious, as this correlation may have been driven by the autocorrelation
375 between WFPS and air temperature (Spearman's $\rho = -0.59$, $P < 0.01$, $n = 33$). In CAF, stem N₂O
376 emissions were only positively correlated with soil N₂O emissions (Table 3).

377 We detected no difference in WFPS between the forest and CAF ($P = 0.15$ – 0.28 ; Table
378 4) at any of the sites. For the CAF, we detected higher WFPS in the wet season compared to the
379 dry season at two sites ($P < 0.01$; Table A3; Fig. 2g, h) whereas there was no seasonal difference



380 in WFPS for the forests at any sites ($P = 0.31\text{--}0.92$; Table A2; Fig. 2g, h, i). At all the three sites,
381 the dominant form of mineral N was NH_4^+ (Table 4). There was generally no difference in soil
382 NH_4^+ and NO_3^- between the wet and dry seasons ($P = 0.12\text{--}0.93$), except for the forests at two
383 sites with larger values in the dry than wet season ($P < 0.01$; Tables S2, S3).

384 3.2 Soil N_2O emissions

385 Soil N_2O emissions did not differ between forest and CAF at any site ($P = 0.06\text{--}0.86$; Table 2).
386 Similarly, no differences in soil N_2O emissions were detected among sites for each land use ($P =$
387 $0.26\text{--}0.44$; Table 2). Soil N_2O emissions exhibited consistent seasonal patterns with larger fluxes
388 in the wet than dry season for both land uses (all $P < 0.01$; Tables S2, S3; Fig. 2d, e, f).

389 Over the measurement period, soil N_2O emissions from the forests were positively
390 correlated with soil-air N_2O concentrations and negatively correlated with NH_4^+ contents (Table
391 3). In the CAF, soil N_2O emissions were positively correlated with WFPS and soil-air N_2O
392 concentrations, and negatively correlated with air temperatures (Table 3). We did not detect any
393 correlation between annual total N_2O fluxes and soil physical and biochemical characteristics.
394 This was not surprising as the ranges of these soil characteristics were relatively small among
395 sites, which reduce the likelihood that significant correlations will be detected.

396 3.3 Soil biochemical characteristics

397 Soil physical characteristics (clay content, bulk density) did not differ between forest and CAF
398 at any of the sites (Table 1). Across sites, Biba Yezoum had lower clay content compared to the
399 other sites for each land use ($P < 0.01$). Generally, the forest showed higher SOC and total N
400 compared to the CAF ($P < 0.01\text{--}0.05$; Table 1). Soil ^{15}N natural abundance signatures, as an
401 index of the long-term soil N availability, were generally similar between the forest and CAF
402 except at Aloum site ($P < 0.01$; Table 1). Soil C/N ratio, another proxy for the long-term soil N
403 status, was higher in the forest than in the CAF at all sites ($P < 0.01\text{--}0.05$). Soil pH and



404 exchangeable bases were lower in the forest compared to the CAF at all sites and the converse
405 was true for exchangeable Al ($P < 0.01$ – 0.05 ; Table 1). Soil ECEC did not differ between the
406 land uses at two sites ($P < 0.01$; Table 1) and all were low congruent to Ferralsol soils.

407 **4 Discussion**

408 **4.1 Stem and soil N₂O emissions from the forest**

409 There has been no study on tree stem N₂O emission from Africa, nor has any study been reported
410 for the Congo Basin on soil N₂O emission with year-round measurements and spatial replication.
411 Stems consistently emitted N₂O in both land uses (Table 2; Fig 1, Fig. 2a, b, c), exemplifying that
412 tropical trees on well-drained soils were important contributors of ecosystem N₂O emission. So
413 far, there are only two tree species of tropical lowland forest reported with measurements of stem
414 N₂O emissions (Welch et al., 2019). Our present study included 23 tree species and their
415 comparable stem N₂O emissions, at least from highly weathered Ferralsol soils, across sites over
416 a year of measurements provided support to our spatial extrapolation based on DBH of trees in
417 the sites. Mean stem N₂O fluxes from our study were within the range of those reported for
418 temperate forests (0.01 – $2.2 \mu\text{g N m}^{-2} \text{ stem h}^{-1}$; Díaz-Pinés et al., 2016; Machacova et al., 2016;
419 Wen et al., 2017), but substantially lower than the reported stem N₂O emissions of 51 – $759 \mu\text{g N}$
420 $\text{m}^{-2} \text{ stem h}^{-1}$ for a humid forest in Panama (Welch et al., 2019). However, Welch et al. (2019)
421 measured stem N₂O emissions at a lower stem height (0.3 m) compared to our study (1.3 m),
422 which may partly explain their much larger N₂O emissions, as another study reported that larger
423 N₂O emissions occur nearer to the stem base of trees (Barba et al., 2019). Moreover, the
424 consistently higher stem than soil N₂O emissions found by Welch et al. (2019), which we did not
425 observe in our study, may point to production of N₂O within the stem (e.g., Lenhart et al., 2019).
426 Nonetheless, such high stem N₂O emissions as reported by Welch et al. (2019) have not been
427 observed anywhere else under field conditions.



428 Our annual soil N₂O emissions from forests (Table 2) were lower than the reported global
429 average for humid tropical forests (2.81 kg N ha⁻¹ yr⁻¹; summarised by Castaldi et al., 2013). In
430 contrast, the N₂O emissions from our forest soils were comparable to those reported for lowland
431 forests on Ferralsol soils in Panama (0.35–1.07 kg N ha⁻¹ yr⁻¹; Matson et al., 2017), and lowland
432 forests on Acrisol soils in Indonesia (0.9 and 1.0 kg N ha⁻¹ yr⁻¹; Hassler et al., 2017). These were
433 possibly due to the generally similar soil N availability in our forest sites as these forest sites in
434 Panama and Indonesia, indicated by their comparable soil mineral N contents and soil ¹⁵N natural
435 abundance signatures.

436 In comparison with studies from sub-Saharan Africa, annual soil N₂O emissions from our
437 forests were lower than the annual N₂O emissions reported for the Mayombe forest in Congo (2.9
438 kg N ha⁻¹ yr⁻¹; Serca et al., 1994), Kakamega mountain rainforest in Kenya (2.6 kg N ha⁻¹ yr⁻¹;
439 Werner et al., 2007b), and Ankasa rainforest in Ghana (2.3 kg N ha⁻¹ yr⁻¹; Castaldi et al., 2013),
440 but similar in magnitude as those reported for Mau Afromontane forest in Kenya (1.1 kg N ha⁻¹
441 yr⁻¹; Wanyama et al., 2018). Although these African sites have similar precipitation level and
442 highly weathered acidic soils as our study sites, the Kakamega rainforest in Kenya had higher
443 SOC (7.9–20 %) and N contents (0.5–1.6 %) in the topsoil layer compared to our forest sites
444 (2.8–4.7 % SOC, 0.2–0.4 % total N), which may explain its correspondingly higher soil N₂O
445 emissions. The study in Congo (Serca et al., 1994), however, was conducted only in a short
446 campaign (two rainy months and one dry month) with less sampling frequency and spatial
447 replication, which may not be a good representation of the spatial and temporal dynamics of soil
448 N₂O fluxes to achieve annual and large-scale estimate.



449 **4.2 Source of tree stem N₂O emissions and their contribution to total (stem + soil) N₂O**
450 **emissions**

451 Emitted N₂O from stems were found to originate predominantly from N₂O produced in the soil,
452 as shown by the ¹⁵N tracing experiment (Fig. 3). Additionally, the positive correlations of stem
453 N₂O emissions with soil-air N₂O concentrations and soil N₂O emissions (Table 3) suggest that
454 the seasonal variation in stem N₂O emissions (Table A2; Fig. 2) was likely driven by the temporal
455 dynamics of produced N₂O in the soil, which partly supported our second hypothesis. While there
456 has been suggestions of within-tree N₂O production (e.g., Lenhart et al., 2019), our finding from
457 the ¹⁵N tracing experiment, combined with the correlations of stem N₂O emissions with VPD and
458 air temperature, pointed to a transport mechanism of dissolved N₂O in soil water by transpiration
459 stream, which has been reported to be important for upland trees that do not have aerenchyma
460 (Machacova et al., 2016; Welch et al., 2019; Wen et al., 2017).

461 The contributions of up-scaled stem N₂O emissions from our studied forests to total (stem
462 + soil) N₂O emissions (Table 2) were higher than those reported for temperate forests (1–18 %;
463 Díaz-Pinés et al., 2016; Machacova et al., 2016; Wen et al., 2017). Given the higher stem N₂O
464 emissions in the wet than dry seasons (Table A2), coupled with the fact that we consistently
465 measured positive fluxes or net stem N₂O emissions throughout our measurement period (Fig. 2),
466 we conclude that tree stems in these well-drained Ferralsol soils were efficient conduits for
467 releasing N₂O from the soil. This has significant implications especially during the rainy season
468 as this pathway bypasses the chance for complete denitrification (N₂O to N₂ reduction) in the
469 soil.

470 **4.3 Factors controlling temporal variability of stem and soil N₂O fluxes**

471 The positive correlation of stem N₂O emissions with VPD and air temperature in the forest
472 suggests for transport of N₂O via sap flow, for which the latter had been shown to be stimulated



473 with increasing VPD and air temperature (McJannet et al., 2007; O'Brien et al., 2004). Soil water
474 containing dissolved N₂O is transported through the xylem via the transpiration stream and
475 eventually emitted from the stem surface to the atmosphere (Díaz-Pinés et al., 2016; Welch et al.,
476 2019; Wen et al., 2017).

477 Soil moisture has been shown to affect strongly the seasonal variation of soil N₂O
478 emissions from tropical ecosystems, with increases in soil N₂O emissions by predominantly
479 denitrification process at high WFPS (Corre et al., 2014; Koehler et al., 2009; Matson et al., 2017;
480 Werner et al., 2006). The larger stem N₂O emissions from the forest and soil N₂O emissions from
481 both land uses in the wet than the dry seasons (Tables S2, S3) signified the favourable soil N₂O
482 production during the wet season, which suggests that denitrification was the dominant N₂O-
483 producing process. However, the moderate WFPS across the year (Table 4) suggests that
484 nitrification may also have contributed to N₂O emissions, especially at Biba Yezoum (with lower
485 rainfall and clay contents; Tables 1, S1) where the low WFPS (Table 4) likely favoured
486 nitrification (Corre et al., 2014). For the forest, the negative correlation of the stem and soil N₂O
487 emissions with soil NH₄⁺ (Tables 3, S2) may be indicative of a conservative soil N cycle in our
488 forest sites, as supported by the dominance of soil NH₄⁺ over NO₃⁻ (Table 2) and by the lower
489 soil N₂O emissions at our sites compared to NO₃⁻-dominated systems (Davidson et al., 2000).
490 Although the soil mineral N content alone does not indicate the N-supplying capacity of the soil,
491 the relative contents of NH₄⁺ over NO₃⁻ can be a good indicator of whether the soil N cycling is
492 conservative with low N₂O losses or increasingly leaky (Corre et al., 2010, 2014).

493 **4.4 Land-use change effects on soil N₂O emissions**

494 The annual soil N₂O emissions from CAF (Table 2) were comparable with those reported for
495 rubber agroforestry in Indonesia (0.6–1.2 kg N ha⁻¹ yr⁻¹; Hassler et al., 2017) and from multistrata
496 agroforestry systems in Peru (0.6 kg N ha⁻¹ yr⁻¹; Palm et al., 2002). However, our soil N₂O
497 emissions from CAF were higher than those from an extensively managed homegarden in



498 Tanzania ($0.35 \text{ N ha}^{-1} \text{ yr}^{-1}$; Gütlein et al., 2018). In a review, Kim et al. (2016a) reported mean
499 annual N_2O emission from agroforestry systems to be $7.7 \text{ kg N ha}^{-1} \text{ yr}^{-1}$. Most of the data used
500 in their review were from intensively managed agroforestry systems with varied fertilizer inputs,
501 which were absent in our extensively managed CAF systems. In line with this, our measured soil
502 N_2O emissions from the CAF were also lower than the emissions reported for 10–23 year old
503 CAF in Indonesia ($3.1 \text{ kg N ha}^{-1} \text{ yr}^{-1}$; Veldkamp et al., 2008). Our measured N_2O emissions
504 provide the first estimates for traditional CAF systems in Africa, as these production systems
505 were not represented in extrapolation of GHG budgets despite their extensive coverage in Africa.

506 Soil N_2O emissions did not differ between forest and CAF systems, which supported our
507 first hypothesis. This is possibly due to the presence of leguminous trees in both systems (Table
508 A1), which can compensate for N export from harvest and other losses (Erickson et al., 2002;
509 Veldkamp et al., 2008). Although studies have hinted on increased N_2O emissions from managed
510 systems that utilize leguminous trees as cover crops (Veldkamp et al., 2008), the similar
511 abundance of leguminous trees between forest and CAF at our sites may have offset this effect
512 (Table A1). Previous studies have indeed reported similar soil N_2O fluxes between reference
513 forests and unfertilized agroforestry systems (Van Lent et al., 2015). Despite the general absence
514 of heavy soil physical disturbance, cultivation and fertilization in these traditional CAF systems,
515 some soil biochemical characteristics have decreased (Table 1); however, these did not translate
516 into detectable differences in soil N_2O emissions with those from forest.

517 **4.5 Implications**

518 The biophysical conditions of our forest sites were representative of approximately two-thirds of
519 the rainforest area in the Congo Basin ($1.137 \times 10^6 \text{ km}^2$; Fig. B3), considering the same Ferralsol
520 soils, similar elevation ($\leq 1000 \text{ m asl}$), and annual rainfall between 1,500 and 2,100 mm yr^{-1} .
521 Using the total (soil + stem) N_2O emission from our forest sites ($1.55 \pm 0.20 \text{ N}_2\text{O-N kg ha}^{-1} \text{ yr}^{-1}$;
522 Table 2), our extrapolated emission for the two-thirds of the Congo Basin was $0.18 \pm 0.05 \text{ Tg}$



523 $\text{N}_2\text{O-N yr}^{-1}$ (error estimate is the 95 % confidence interval). This accounted 52 % of the earlier
524 estimate of soil N_2O emissions from tropical rainforests in Africa ($0.34 \text{ Tg N}_2\text{O-N yr}^{-1}$; Werner
525 et al., 2007), or 25 % based on the more recent estimate ($0.72 \text{ Tg N}_2\text{O-N yr}^{-1}$; Valentini et al.,
526 2014). We acknowledge, however, that there are uncertainties in our extrapolation (as is the case
527 of these cited estimates) because our up-scaling approach from plot to regional level did not
528 account for the spatial variability of large-scale drivers of soil N_2O emissions, such as soil texture,
529 landforms and vegetation characteristics (e.g., Corre et al., 1999). These limitations of our
530 estimate of N_2O source strength for the Congo Basin rainforests call for further investigations in
531 Africa to address the geographic bias of studies in the tropical region (e.g., Powers et al., 2011).

532 Our year-round measurements of stem and soil N_2O fluxes were the first detailed study
533 carried out in the Congo Basin, with key implications on improved estimates of N_2O budget for
534 Africa. Our results revealed that trees on well-drained, highly weathered soils served as an
535 important N_2O emission pathway, with the potential to overlook up to 38 % of N_2O emissions if
536 trees are not considered in the ecosystem N_2O budget. Additionally, forest conversion to
537 traditional, mature (>20 years old) CAF systems had no effect on stem and soil N_2O emissions,
538 because of similarities in soil moisture and soil texture, absence of fertilizer application, and
539 comparable abundance of leguminous trees in both land uses, which can compensate for N export
540 from harvest or other losses. Further multi-temporal and spatially replicated studies are needed
541 to provide additional insights on the effect of forest conversion to other land uses on GHG fluxes
542 from the African continent in order to improve GHG budget estimations for the region.

543 *Data availability.* Data available from the Göttingen Research Online repository: Iddris, N. A.,
544 Corre, M. D., Yemefack, M., van Straaten, O. and Veldkamp, E.: Stem and soil nitrous oxide
545 fluxes from rainforest and cacao agroforest on highly weathered soils in the Congo Basin, ,
546 <https://doi.org/10.25625/T2CGYM>, 2020.



547 *Author Contributions.* EV and MDC conceived the research project; NAI carried out fieldwork
548 and analyzed data; NAI and OvS performed GIS analysis; NAI and MDC interpreted data and
549 wrote the manuscript; EV, OvS and MY revised the draft manuscript.

550 *Competing interests.* The authors declare that they have no conflict of interest.

551 *Acknowledgements.* This study was funded by the German Research Foundation (DFG, VE
552 219/14-1, STR 1375/1-1). We gratefully acknowledge our counterparts in Cameroon, the
553 International Institute for Tropical Agriculture (IITA) for granting us access and use of their
554 storage facilities. We are especially grateful to our Cameroonian field assistants Leonel Boris
555 Gadjuj Youatou, Narcis Lekeng, Yannick Eyenga Alfred, Denis Djiyo and all the field workers
556 for their great support with field measurements, as well as Raphael Manu for helping with the
557 GIS work and Rodine Tchifofo Lontsi for many discussions on soil processes and Cameroonian
558 settings. We also thank the village leaders and local plot owners for granting us access to their
559 forest and cacao farms. We thank Andrea Bauer, Kerstin Langs, Martina Knaust and Lars Szewc
560 for their assistance with laboratory analyses.

561 **References**

562 Allen, R. G., Pereira, L. S., Raes, D. and Smith, M.: Determination of ET_0 , crop
563 evapotranspiration, Guidel. Comput. Crop Water Requir. Irrig. Drain. Pap. 56, 309 [online]
564 Available from: http://www.hidmet.gov.rs/podaci/agro/table_of_contents_files.pdf, 1998.

565 Barba, J., Poyatos, R. and Vargas, R.: Automated measurements of greenhouse gases fluxes
566 from tree stems and soils: magnitudes, patterns and drivers, *Sci. Rep.*, 9(1), 1–13,
567 doi:10.1038/s41598-019-39663-8, 2019.

568 Bouwman, A. F., Van Der Hoek, K. W. and Olivier, J. G. J.: Uncertainties in the global source
569 distribution of nitrous oxide, *J. Geophys. Res.*, 100(D2), 2785–2800,
570 doi:10.1029/94JD02946, 1995.



- 571 Breuer, L., Papen, H. and Butterbach-Bahl, K.: N₂O emission from tropical forest soils of
572 Australia, *J. Geophys. Res. Atmos.*, 105(D21), 26353–26367, doi:10.1029/2000JD900424,
573 2000.
- 574 Castaldi, S., Bertolini, T., Valente, A., Chiti, T. and Valentini, R.: Nitrous oxide emissions from
575 soil of an African rain forest in Ghana, *Biogeosciences*, 10(6), 4179–4187, doi:10.5194/bg-
576 10-4179-2013, 2013.
- 577 Climate-Data.org: Cameroon climate, [online] Available from: <https://en.climate->
578 [data.org/africa/cameroon-142/](https://en.climate-data.org/africa/cameroon-142/) (Accessed 21 May 2019), 2019.
- 579 Corre, M. D., Pennock, D. J., Van Kessel, C. and Elliott, D. K.: Estimation of annual nitrous
580 oxide emissions from a transitional grassland-forest region in Saskatchewan, Canada,
581 *Biogeochemistry*, 44(1), 29–49, doi:10.1023/A:1006025907180, 1999.
- 582 Corre, M. D., Dechert, G. and Veldkamp, E.: Soil nitrogen cycling following montane forest
583 conversion in Central Sulawesi, Indonesia, *Soil Sci. Soc. Am. J.*, 70(2), 359–366,
584 doi:10.2136/sssaj2005.0061, 2006.
- 585 Corre, M. D., Veldkamp, E., Arnold, J. and Joseph Wright, S.: Impact of elevated N input on
586 soil N cycling and losses in old-growth lowland and montane forests in Panama, *Ecology*,
587 91(6), 1715–1729, doi:10.1890/09-0274.1, 2010.
- 588 Corre, M. D., Sueta, J. P. and Veldkamp, E.: Nitrogen-oxide emissions from tropical forest soils
589 exposed to elevated nitrogen input strongly interact with rainfall quantity and seasonality,
590 *Biogeochemistry*, 118(1–3), 103–120, doi:10.1007/s10533-013-9908-3, 2014.
- 591 Crawley, M. J.: *The R Book*, John Wiley & Sons Ltd, Chichester, UK., 2009.
- 592 Curtis, J. T. and McIntosh, R. P.: An Upland Forest Continuum in the Prairie-Forest Border
593 Region of Wisconsin, *Ecology*, 32(3), 476–496, doi:10.2307/1931725, 1951.
- 594 Davidson, E. A. and Kanter, D.: Inventories and scenarios of nitrous oxide emissions, *Environ.*
595 *Res. Lett.*, 9(10), doi:10.1088/1748-9326/9/10/105012, 2014.



- 596 Davidson, E. A. and Verchot, L. V.: Testing the hole-in-the-pipe model of nitric and nitrous
597 oxide emissions from soils using the TRAGNET database, *Global Biogeochem. Cycles*,
598 14(4), 1035–1043, doi:10.1029/1999GB001223, 2000.
- 599 Davidson, E. A., Keller, M., Erickson, H. E., Verchot, L. V. and Veldkamp, E.: Testing a
600 Conceptual Model of Soil Emissions of Nitrous and Nitric Oxides, *Bioscience*, 50(8), 667,
601 doi:10.1641/0006-3568(2000)050[0667:tacmos]2.0.co;2, 2000.
- 602 Denman, K. L., Brasseur, G., Chidthaisong, A., Ciais, P., Cox, P. M., Dickinson, R. E.,
603 Hauglustaine, D., Heinze, C., Holland, E., Jacob, D., Lohmann, U., Ramachandran, S., da
604 Silva Dias, P. L., Wofsy, S. C. and Zhang, X.: Couplings Between Changes in the Climate
605 System and Biogeochemistry, in *Climate Change 2007: The Physical Science Basis*.
606 Contribution of Working Group I to the Fourth Assessment Report of the Intergovernmental
607 Panel on Climate Change, Cambridge University Press, Cambridge, United Kingdom and
608 New York, NY, USA. [online] Available from:
609 <https://www.ipcc.ch/site/assets/uploads/2018/02/ar4-wg1-chapter7-1.pdf>, 2007.
- 610 Díaz-Pinés, E., Heras, P., Gasche, R., Rubio, A., Rennenberg, H., Butterbach-Bahl, K. and
611 Kiese, R.: Nitrous oxide emissions from stems of ash (*Fraxinus angustifolia* Vahl) and
612 European beech (*Fagus sylvatica* L.), *Plant Soil*, 398(1–2), 35–45,
613 doi:<https://doi.org/10.1007/s11104-015-2629-8>, 2016.
- 614 Dkamela, G. P.: The context of REDD+ in Cameroon: Drivers, agents and institutions,
615 Occasional., CIFOR, Bogor, Indonesia., 2010.
- 616 Erickson, H. E., Davidson, E. A. and Keller, M.: Former land-use and tree species affect
617 nitrogen oxide emissions from a tropical dry forest, *Oecologia*, 130(2), 297–308,
618 doi:10.1007/s004420100801, 2002.
- 619 FAO/IIASA/ISRIC/ISS-CAS/JRC: Harmonized World Soil Database (version 1.2). FAO,
620 Rome, Italy and IIASA, Laxenburg, Austria., [online] Available from:



- 621 <http://webarchive.iiasa.ac.at/Research/LUC/External-World-soil-database/HTML/> (Accessed
622 13 September 2019), 2012.
- 623 Gütlein, A., Gerschlauer, F., Kikoti, I. and Kiese, R.: Impacts of climate and land use on N₂O
624 and CH₄ fluxes from tropical ecosystems in the Mt. Kilimanjaro region, Tanzania, Glob.
625 Chang. Biol., 24, 1239–1255, doi:10.1111/gcb.13944, 2018.
- 626 Gwanfogbe, M., Meligui, A., Moukam, J. and Nguoghia, J.: Geography of Cameroon.,
627 Macmillan Education Ltd, Hong Kong., 1983.
- 628 Hassler, E., Corre, M. D., Tjoa, A., Damris, M., Utami, S. R. and Veldkamp, E.: Soil fertility
629 controls soil-atmosphere carbon dioxide and methane fluxes in a tropical landscape
630 converted from lowland forest to rubber and oil palm plantations, Biogeosciences Discuss.,
631 12(12), 9163–9207, doi:10.5194/bgd-12-9163-2015, 2015.
- 632 Hassler, E., Corre, M. D., Kurniawan, S. and Veldkamp, E.: Soil nitrogen oxide fluxes from
633 lowland forests converted to smallholder rubber and oil palm plantations in Sumatra,
634 Indonesia, Biogeosciences, 14(11), 2781–2798, doi:https://doi.org/10.5194/bg-14-2781-
635 2017, 2017.
- 636 Hijmans, R. J., Cameron, S. E., Parra, J. L., Jones, P. G. and Jarvis, A.: Very high resolution
637 interpolated climate surfaces for global land areas, Int. J. Climatol., 25(15), 1965–1978,
638 doi:10.1002/joc.1276, 2005.
- 639 Huang, J., Golombek, A., Prinn, R. G., Weiss, R. F., Fraser, P. J., Simmonds, P.,
640 Dlugokencky, E. J., Hall, B., Elkins, J., Steele, L. P., Langenfelds, R. L., Krummel, P. B.,
641 Dutton, G. and Porter, L.: Estimation of regional emissions of nitrous oxide from 1997 to
642 2005 using multinetwork measurements, a chemical transport model, and an inverse method,
643 J. Geophys. Res. Atmos., 113(17), 1–19, doi:10.1029/2007JD009381, 2008.
- 644 IUSS Working Group WRB: World Reference Base for Soil Resources 2014, update 2015
645 International soil classification system for naming soils and creating legends for soil maps.



- 646 World Soil Resources Reports No. 106., FAO, Rome., 2015.
- 647 Jarvis, A., Reuter, H. I., Nelson, A. and Guevara, E.: Hole-filled SRTM for the globe, Version
648 4. CGIAR-CSI SRTM 90m Database, Int. Cent. Trop. Agric. Cali, Columbia.
649 <http://srtm.csi.cgiar.org>, (September 2017), 2008.
- 650 Kiese, R., Hewett, B., Graham, A. and Butterbach-Bahl, K.: Seasonal variability of N₂O
651 emissions and CH₄ uptake by tropical rainforest soils of Queensland, Australia, *Global*
652 *Biogeochem. Cycles*, 17(2), 1043, doi:10.1029/2002gb002014, 2003.
- 653 Kim, D. G., Kirschbaum, M. U. F. and Beedy, T. L.: Carbon sequestration and net emissions of
654 CH₄ and N₂O under agroforestry: Synthesizing available data and suggestions for future
655 studies, *Agric. Ecosyst. Environ.*, 226, 65–78, doi:10.1016/j.agee.2016.04.011, 2016a.
- 656 Kim, D. G., Thomas, A. D., Pelster, D. E., Rosenstock, T. S. and Sanz-Cobena, A.: Greenhouse
657 gas emissions from natural ecosystems and agricultural lands in sub-Saharan Africa:
658 Synthesis of available data and suggestions for further research, *Biogeosciences*, 13(16),
659 4789–4809, doi:10.5194/bg-13-4789-2016, 2016b.
- 660 Koehler, B., Corre, M. D., Veldkamp, E., Wullaert, H. and Wright, S. J.: Immediate and long-
661 term nitrogen oxide emissions from tropical forest soils exposed to elevated nitrogen input,
662 *Glob. Chang. Biol.*, 15(8), 2049–2066, doi:10.1111/j.1365-2486.2008.01826.x, 2009.
- 663 Kotto, J. S., Moukam, A., Njomgang, R., Tiki-Manga, T., Tonye, J., Diaw, C., Gockowski, J.,
664 Hauser, S., Weise, S. F., Nwaga, D., Zapfack, L., Palm, C. A., Woome, P., Gillison, A.,
665 Bignell, D. and Tondoh, J.: Alternatives to slash-and-burn in Indonesia: summary report &
666 synthesis of phase II in Cameroon, Nairobi. Kenya., 2002.
- 667 Kreuzwieser, J., Buchholz, J. and Rennenberg, H.: Emission of Methane and Nitrous Oxide by
668 Australian Mangrove Ecosystems, *Plant Biol.*, 5(4), 423–431, doi:10.1055/s-2003-42712,
669 2003.
- 670 Kroetsch, D. and Wang, C.: Particle size distribution, in *Soil Sampling and Methods of*



- 671 Analysis, Second Edition, pp. 713–725., 2008.
- 672 Lenhart, K., Behrendt, T., Greiner, S., Steinkamp, J., Well, R., Giesemann, A. and Keppler, F.:
673 Nitrous oxide effluxes from plants as a potentially important source to the atmosphere, New
674 Phytol., 221(3), 1398–1408, doi:10.1111/nph.15455, 2019.
- 675 Van Lent, J., Hergoualc'H, K. and Verchot, L. V.: Reviews and syntheses: Soil N₂O and NO
676 emissions from land use and land-use change in the tropics and subtropics: A meta-analysis,
677 Biogeosciences, 12(23), 7299–7313, doi:10.5194/bg-12-7299-2015, 2015.
- 678 Machacova, K., Papen, H., Kreuzwieser, J. and Rennenberg, H.: Inundation strongly stimulates
679 nitrous oxide emissions from stems of the upland tree *Fagus sylvatica* and the riparian tree
680 *Alnus glutinosa*, Plant Soil, 364(1–2), 287–301, doi:10.1007/s11104-012-1359-4, 2013.
- 681 Machacova, K., Bäck, J., Vanhatalo, A., Halmeenmäki, E., Kolari, P., Mammarella, I.,
682 Pumpanen, J., Acosta, M., Urban, O. and Pihlatie, M.: *Pinus sylvestris* as a missing source of
683 nitrous oxide and methane in boreal forest, Sci. Rep., 6(March), 1–8, doi:10.1038/srep23410,
684 2016.
- 685 Machacova, K., Maier, M., Svobodova, K., Lang, F. and Urban, O.: Cryptogamic stem covers
686 may contribute to nitrous oxide consumption by mature beech trees, Sci. Rep., 7(1), 1–7,
687 doi:10.1038/s41598-017-13781-7, 2017.
- 688 Matson, A. L., Corre, M. D., Langs, K. and Veldkamp, E.: Soil trace gas fluxes along
689 orthogonal precipitation and soil fertility gradients in tropical lowland forests of Panama,
690 Biogeosciences, 14(14), 3509–3524, doi:10.5194/bg-14-3509-2017, 2017.
- 691 McJannet, D., Fitch, P., Disher, M. and Wallace, J.: Measurements of transpiration in four
692 tropical rainforest types of north Queensland, Australia, Hydrol. Process., 21, 3549–3564,
693 doi:https://doi.org/10.1002/hyp.6576, 2007.
- 694 Müller, A. K., Matson, A. L., Corre, M. D. and Veldkamp, E.: Soil N₂O fluxes along an
695 elevation gradient of tropical montane forests under experimental nitrogen and phosphorus



- 696 addition, *Front. Earth Sci.*, 3(October), 1–12, doi:10.3389/feart.2015.00066, 2015.
- 697 Neill, C., Steudler, P. A., Garcia-Montiel, D. C., Melillo, J. M., Feigl, B. J., Piccolo, M. C. and
698 Cerri, C. C.: Rates and controls of nitrous oxide and nitric oxide emissions following
699 conversion of forest to pasture in Rondônia, *Nutr. Cycl. Agroecosystems*, 71(1), 1–15,
700 doi:10.1007/s10705-004-0378-9, 2005.
- 701 O’Brien, J. J., Oberbauer, S. F. and Clark, D. B.: Whole tree xylem sap flow responses to
702 multiple environmental variables in a wet tropical forest, *Plant, Cell Environ.*, 27(5), 551–
703 567, doi:10.1111/j.1365-3040.2003.01160.x, 2004.
- 704 Palm, C. A., Alegre, J. C., Arevalo, L., Mutuo, P. K., Mosier, A. R. and Coe, R.: Nitrous oxide
705 and methane fluxes in six different land use systems in the Peruvian Amazon, *Global
706 Biogeochem. Cycles*, 16(4), 1073, doi:10.1029/2001gb001855, 2002.
- 707 Powers, J. S., Corre, M. D., Twine, T. E. and Veldkamp, E.: Geographic bias of field
708 observations of soil carbon stocks with tropical land-use changes precludes spatial
709 extrapolation, *Proc. Natl. Acad. Sci. U. S. A.*, 108(15), 6318–6322,
710 doi:10.1073/pnas.1016774108, 2011.
- 711 Purbopuspito, J., Veldkamp, E., Brumme, R. and Murdiyarso, D.: Trace gas fluxes and nitrogen
712 cycling along an elevation sequence of tropical montane forests in Central Sulawesi,
713 Indonesia, *Global Biogeochem. Cycles*, 20(3), 1–11, doi:10.1029/2005GB002516, 2006.
- 714 Ravishankara, A. R., Daniel, J. S. and Portmann, R. W.: Nitrous oxide (N₂O): The dominant
715 ozone-depleting substance emitted in the 21st century, *Science* (80-.), 326(5949), 123–125,
716 doi:10.1126/science.1176985, 2009.
- 717 Rusch, H. and Rennenberg, H.: Black alder (*Alnus glutinosa* (L.) Gaertn.) trees mediate
718 methane and nitrous oxide emission from the soil to the atmosphere, *Plant Soil*, 201(1), 1–7,
719 doi:10.1023/A:1004331521059, 1998.
- 720 Saj, S., Jagoret, P. and Todem Ngogue, H.: Carbon storage and density dynamics of associated



- 721 trees in three contrasting *Theobroma cacao* agroforests of Central Cameroon, *Agrofor. Syst.*,
722 87(6), 1309–1320, doi:10.1007/s10457-013-9639-4, 2013.
- 723 Serca, D., Delmas, R., Jambert, C. and Labroue, L.: Emissions of nitrogen oxides from
724 equatorial rain forest in central Africa., *Tellus B Chem. Phys. Meteorol.*, 46(4), 243–254,
725 doi:10.3402/tellusb.v46i4.15795, 1994.
- 726 Sonwa, D. J., Nkongmeneck, B. A., Weise, S. F., Tchatat, M., Adesina, A. A. and Janssens, M.
727 J. J.: Diversity of plants in cocoa agroforests in the humid forest zone of Southern
728 Cameroon, *Biodivers. Conserv.*, 16(8), 2385–2400, doi:10.1007/s10531-007-9187-1, 2007.
- 729 van Straaten, O., Corre, M. D., Wolf, K., Tchienkoua, M., Cuellar, E., Matthews, R. B. and
730 Veldkamp, E.: Conversion of lowland tropical forests to tree cash crop plantations loses up
731 to one-half of stored soil organic carbon, *Proc. Natl. Acad. Sci.*, 112(32), 9956–9960,
732 doi:10.1073/pnas.1504628112, 2015.
- 733 Tchiofo Lontsi, R., Corre, M. D., van Straaten, O. and Veldkamp, E.: Changes in soil organic
734 carbon and nutrient stocks in conventional selective logging versus reduced-impact logging
735 in rainforests on highly weathered soils in Southern Cameroon, *For. Ecol. Manage.*,
736 451(August), 117522, doi:10.1016/j.foreco.2019.117522, 2019.
- 737 Thompson, R. L., Chevallier, F., Crotwell, A. M., Dutton, G., Langenfelds, R. L., Prinn, R. G.,
738 Weiss, R. F., Tohjima, Y., Nakazawa, T., Krummel, P. B., Steele, L. P., Fraser, P. J.,
739 O’doherly, S., Ishijima, K. and Aoki, S.: Nitrous oxide emissions 1999 to 2009 from a global
740 atmospheric inversion, *Atmos. Chem. Phys.*, 14(4), 1801–1817, doi:10.5194/acp-14-1801-
741 2014, 2014.
- 742 Valentini, R., Arneth, A., Bombelli, A., Castaldi, S., Cazzolla Gatti, R., Chevallier, F., Ciais, P.,
743 Grieco, E., Hartmann, J., Henry, M., Houghton, R. A., Jung, M., Kutsch, W. L., Malhi, Y.,
744 Mayorga, E., Merbold, L., Murray-Tortarolo, G., Papale, D., Peylin, P., Poulter, B.,
745 Raymond, P. A., Santini, M., Sitch, S., Vaglio Laurin, G., Van Der Werf, G. R., Williams, C.



- 746 A. and Scholes, R. J.: A full greenhouse gases budget of africa: Synthesis, uncertainties, and
747 vulnerabilities, *Biogeosciences*, 11(2), 381–407, doi:10.5194/bg-11-381-2014, 2014.
- 748 Veldkamp, E.: Organic Carbon Turnover in Three Tropical Soils under Pasture after
749 Deforestation, *Soil Sci. Soc. Am. J.*, 58(1), 175–180,
750 doi:10.2136/sssaj1994.03615995005800010025x, 1994.
- 751 Veldkamp, E., Purbopuspito, J., Corre, M. D., Brumme, R. and Murdiyarso, D.: Land use
752 change effects on trace gas fluxes in the forest margins of Central Sulawesi, Indonesia, *J.*
753 *Geophys. Res. Biogeosciences*, 113(2), 1–11, doi:10.1029/2007JG000522, 2008.
- 754 Veldkamp, E., Koehler, B. and Corre, M. D.: Indications of nitrogen-limited methane uptake in
755 tropical forest soils, *Biogeosciences*, 10(8), 5367–5379, doi:10.5194/bg-10-5367-2013,
756 2013.
- 757 Verchot, L. V., Hutabarat, L., Hairiah, K. and van Noordwijk, M.: Nitrogen availability and soil
758 N₂O emissions following conversion of forests to coffee in southern Sumatra, *Global*
759 *Biogeochem. Cycles*, 20(4), 1–12, doi:10.1029/2005GB002469, 2006.
- 760 Wanyama, I., Pelster, D. E., Arias-Navarro, C., Butterbach-Bahl, K., Verchot, L. V. and Rufino,
761 M. C.: Management intensity controls soil N₂O fluxes in an Afromontane ecosystem, *Sci.*
762 *Total Environ.*, 624(December), 769–780, doi:10.1016/j.scitotenv.2017.12.081, 2018.
- 763 Welch, B., Gauci, V. and Sayer, E. J.: Tree stem bases are sources of CH₄ and N₂O in a tropical
764 forest on upland soil during the dry to wet season transition, *Glob. Chang. Biol.*, 25(1), 361–
765 372, doi:10.1111/gcb.14498, 2019.
- 766 Wen, Y., Corre, M. D., Rachow, C., Chen, L. and Veldkamp, E.: Nitrous oxide emissions from
767 stems of alder, beech and spruce in a temperate forest, *Plant Soil*, doi:10.1007/s11104-017-
768 3416-5, 2017.
- 769 Werner, C., Zheng, X., Tang, J., Xie, B., Liu, C., Kiese, R. and Butterbach-Bahl, K.: N₂O, CH₄
770 and CO₂ emissions from seasonal tropical rainforests and a rubber plantation in Southwest



- 771 China, *Plant Soil*, 289(1–2), 335–353, doi:10.1007/s11104-006-9143-y, 2006.
- 772 Werner, C., Butterbach-Bahl, K., Haas, E., Hickler, T. and Kiese, R.: A global inventory of
773 N₂O emissions from tropical rainforest soils using a detailed biogeochemical model, *Global*
774 *Biogeochem. Cycles*, 21(3), doi:10.1029/2006GB002909, 2007a.
- 775 Werner, C., Kiese, R. and Butterbach-Bahl, K.: Soil-atmosphere exchange of N₂O, CH₄, and
776 CO₂ and controlling environmental factors for tropical rain forest sites in western Kenya, *J.*
777 *Geophys. Res.*, 112(3), D03308, doi:10.1029/2006JD007388, 2007b.
- 778 Wolf, K., Veldkamp, E., Homeier, J. and Martinson, G. O.: Nitrogen availability links forest
779 productivity, soil nitrous oxide and nitric oxide fluxes of a tropical montane forest in
780 southern Ecuador, *Global Biogeochem. Cycles*, 25(4), GB4009,
781 doi:10.1029/2010GB003876, 2011.
- 782 Zapfack, L., Engwald, S., Sonké, B., Achoundong, G. and Madong, B. A.: The impact of land
783 conversion on plant biodiversity in the forest zone of Cameroon, *Biodivers. Conserv.*,
784 11(11), 2047–2061, doi:<https://doi.org/10.1023/A:1020861925294>, 2002.



Tables

785 **Table 1.** Mean (\pm SE, $n = 4$) soil biochemical characteristics in the top 50 cm^a depth in forest and
 786 cacao agroforestry (CAF) within each site in the Congo Basin, Cameroon. Means followed by
 787 different lowercase letters indicate significant differences between land-use types within each site
 788 and different capital letters indicate significant differences among the three sites within a land-
 789 use type (Anova with Tukey's HSD test or Kruskal-Wallis ANOVA with multiple comparison
 790 extension test at $P \leq 0.05$).

Soil characteristics	Aloum site		Biba Yezoum site		Tomba site	
	Forest	CAF	Forest	CAF	Forest	CAF
Clay (30-50 cm) (%)	66.0 \pm 2.4 ^{a,A}	59.3 \pm 6.1 ^{a,A}	32.8 \pm 9.4 ^{a,B}	39.5 \pm 0.9 ^{a,B}	55.3 \pm 0.5 ^{a,AB}	51.8 \pm 1.1 ^{a,AB}
Bulk density (g cm ⁻³)	1.2 \pm 0.1 ^{a,A}	1.2 \pm 0.1 ^{a,A}	1.2 \pm 0.1 ^{a,A}	1.2 \pm 0.1 ^{a,A}	1.2 \pm 0.1 ^{a,A}	1.2 \pm 0.1 ^{a,A}
pH (1:4 H ₂ O)	3.7 \pm 0.0 ^{b,A}	4.1 \pm 0.1 ^{a,A}	3.7 \pm 0.1 ^{b,A}	4.6 \pm 0.2 ^{a,A}	3.6 \pm 0.0 ^{b,A}	4.5 \pm 0.2 ^{a,A}
¹⁵ N natural abundance (‰)	8.4 \pm 0.2 ^{b,A}	10.2 \pm 0.1 ^{a,A}	8.6 \pm 0.2 ^{a,A}	9.1 \pm 0.2 ^{a,B}	8.8 \pm 0.1 ^{a,A}	8.8 \pm 0.1 ^{a,B}
Soil organic C (kg C m ⁻²)	12.1 \pm 0.4 ^{a,A}	6.7 \pm 0.2 ^{b,A}	7.2 \pm 0.9 ^{a,B}	5.6 \pm 0.7 ^{a,A}	9.8 \pm 0.2 ^{a,AB}	7.1 \pm 0.4 ^{b,A}
Total N (kg N m ⁻²)	1.1 \pm 0.1 ^{a,A}	0.7 \pm 0.0 ^{b,A}	0.7 \pm 0.1 ^{a,A}	0.5 \pm 0.0 ^{a,B}	0.9 \pm 0.0 ^{a,A}	0.7 \pm 0.0 ^{b,A}
ECEC ^b (mmol _c kg ⁻¹)	57.5 \pm 3.9 ^{a,A}	33.9 \pm 2.8 ^{b,A}	49.1 \pm 11.3 ^{a,A}	41.1 \pm 7.2 ^{a,A}	58.5 \pm 2.0 ^{a,A}	46.8 \pm 4.7 ^{a,A}
Exch. bases ^b (mmol _c kg ⁻¹)	3.5 \pm 0.3 ^{b,B}	8.7 \pm 1.7 ^{a,B}	8.5 \pm 1.1 ^{b,A}	31.0 \pm 8.5 ^{a,A}	9.3 \pm 0.8 ^{b,A}	30.4 \pm 7.6 ^{a,A}
Exchangeable Al (mmol _c kg ⁻¹)	47.3 \pm 3.1 ^{a,A}	20.9 \pm 3.5 ^{b,A}	32.9 \pm 8.9 ^{a,A}	5.4 \pm 1.2 ^{b,B}	39.2 \pm 2.3 ^{a,A}	12.3 \pm 2.7 ^{b,AB}

791 ^a Values are depth-weighted average, except for clay content (30–50 cm) and stocks of soil
 792 organic C and total N, which are sum of the entire 50-cm depth. ^b ECEC: effective cation
 793 exchange capacity; Exch. bases: sum of exchangeable Ca, Mg, K, Na.



794 **Table 2.** Mean (\pm SE, $n = 4$) stem and soil N₂O emission as well as annual stem, soil, and total
 795 (soil + stem) N₂O fluxes from forest and cacao agroforestry (CAF) within each site in the Congo
 796 Basin, Cameroon. Means followed by different lowercase letters indicate significant differences
 797 between land-use types within each site and different capital letters indicate significant
 798 differences among the three sites within a land-use type (linear mixed-effect models with
 799 Tukey's HSD at $P \leq 0.05$).

Site/ Land-use type	Stem N ₂ O fluxes ($\mu\text{g N}$ m^{-2} stem h^{-1})	Annual stem N ₂ O fluxes ^a (kg N ha^{-1} yr^{-1})	Soil N ₂ O fluxes ($\mu\text{g N}$ m^{-2} soil h^{-1})	Annual soil N ₂ O fluxes ^a (kg N ha^{-1} yr^{-1})	Total (soil + stem) N ₂ O flux (kg N ha^{-1} yr^{-1})	Contribution of stem to total N ₂ O flux (%)
Aloum						
Forest	$1.13 \pm 0.22^{\text{a,A}}$	0.13 ± 0.00	$13.7 \pm 2.2^{\text{a,A}}$	0.87 ± 0.14	1.00 ± 0.14	13.7 ± 1.8
CAF	$0.90 \pm 0.16^{\text{a,A}}$	0.09 ± 0.01 (0.02 ± 0.01)	$15.2 \pm 2.8^{\text{a,A}}$	1.06 ± 0.17	1.15 ± 0.17	7.8 ± 1.6
Biba Yezoum						
Forest	$2.38 \pm 0.48^{\text{a,A}}$	0.87 ± 0.05	$17.2 \pm 2.9^{\text{a,A}}$	1.46 ± 0.23	2.33 ± 0.24	38.2 ± 3.5
CAF	$1.11 \pm 0.21^{\text{a,A}}$	0.12 ± 0.01 (0.03 ± 0.01)	$10.6 \pm 2.1^{\text{a,A}}$	0.80 ± 0.20	0.92 ± 0.20	14.8 ± 3.0
Tomba						
Forest	$0.89 \pm 0.10^{\text{a,A}}$	0.14 ± 0.01	$15.0 \pm 1.7^{\text{a,A}}$	1.18 ± 0.18	1.31 ± 0.18	11.4 ± 2.2
CAF	$0.90 \pm 0.12^{\text{a,A}}$	0.12 ± 0.00 (0.05 ± 0.02)	$15.8 \pm 2.0^{\text{a,A}}$	1.25 ± 0.14	1.37 ± 0.14	8.9 ± 0.9

800 ^a Annual stem and soil N₂O fluxes were not statistically tested for differences among sites or
 801 between land-use types since these annual values are trapezoidal extrapolations. Annual stem
 802 N₂O emissions in parentheses are from cacao trees only.



803 **Table 3.** Spearman correlation coefficients of stem N₂O flux ($\mu\text{g N m}^{-2} \text{ stem h}^{-1}$) and soil N₂O
 804 flux ($\mu\text{g N m}^{-2} \text{ soil h}^{-1}$) with air temperature ($^{\circ}\text{C}$), water-filled pore space (WFPS) (%), top 5
 805 cm depth), extractable NH₄⁺ (mg N kg⁻¹, top 5 cm depth), soil-air N₂O concentration (ppm N₂O
 806 at 50 cm depth), and vapour pressure deficit (VPD) (kPa), using the monthly means of the four
 807 replicate plots per land use across the three sites from May 2017 to April 2018 ($n = 33$).

Land use	Variable	Soil N ₂ O flux	Air temp.	WFPS	NH ₄ ⁺	Soil-air N ₂ O concentration	VPD
Forest	Stem N ₂ O flux	0.25	0.39 ^b	-0.41 ^b	-0.57 ^a	0.41 ^b	0.62 ^a
	Soil N ₂ O flux		-0.07	0.15	-0.43 ^b	0.55 ^a	-0.01
CAF	Stem N ₂ O flux	0.60 ^a	-0.29	0.17	-0.26	0.21	0.21
	Soil N ₂ O flux		-0.34 ^b	0.53 ^a	-0.14	0.51 ^a	0.10

^b $P \leq 0.05$, ^a $P \leq 0.01$.



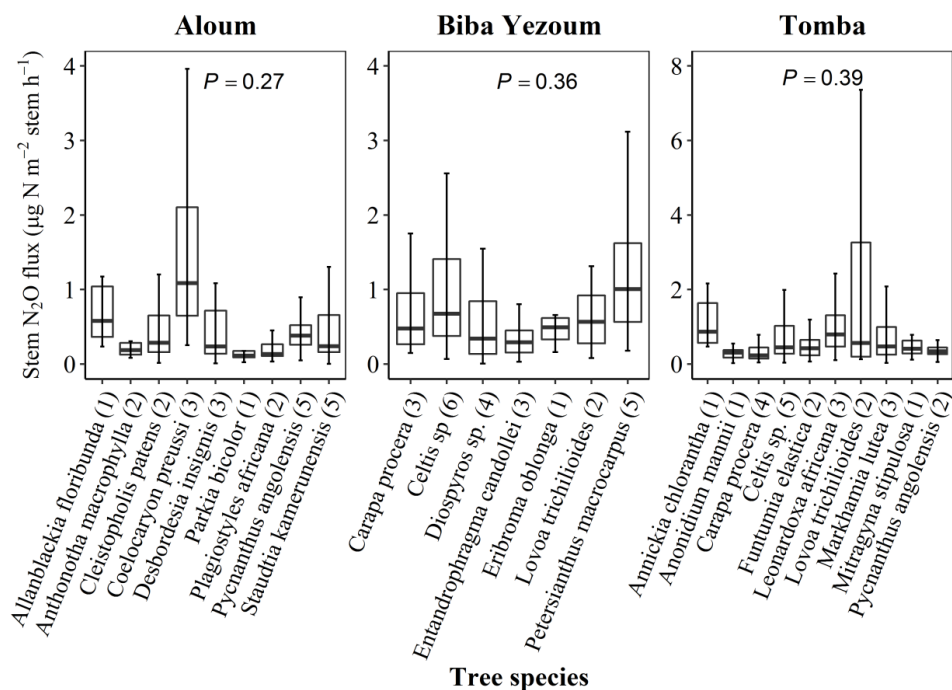
808 **Table 4.** Mean (\pm SE, $n = 4$) water-filled pore space (WFPS) and extractable mineral N in the
 809 top 5 cm of soil in forest and cacao agroforestry (CAF) within each site in Congo Basin,
 810 Cameroon, measured monthly from May 2017 to April 2018.

Site/ Land-use type ^a	WFPS (%)	NH ₄ ⁺ (mg N kg ⁻¹)	NO ₃ ⁻ (mg N kg ⁻¹)
Aloum			
Forest	64.3 \pm 3.6 ^{a,A}	7.3 \pm 1.0 ^{a,A}	6.3 \pm 1.2 ^{a,A}
CAF	56.4 \pm 2.5 ^{a,A}	5.1 \pm 0.8 ^{a,B}	2.4 \pm 0.6 ^{b,A}
Biba Yezoum			
Forest	41.5 \pm 2.7 ^{a,B}	4.9 \pm 0.4 ^{b,B}	2.9 \pm 0.5 ^{a,B}
CAF	32.6 \pm 2.7 ^{a,B}	7.3 \pm 0.4 ^{a,A}	2.7 \pm 0.6 ^{a,A}
Tomba			
Forest	48.3 \pm 3.0 ^{a,B}	7.6 \pm 0.6 ^{a,A}	5.8 \pm 1.0 ^{a,A}
CAF	52.3 \pm 5.1 ^{a,A}	7.1 \pm 0.6 ^{a,A}	2.8 \pm 0.6 ^{b,A}

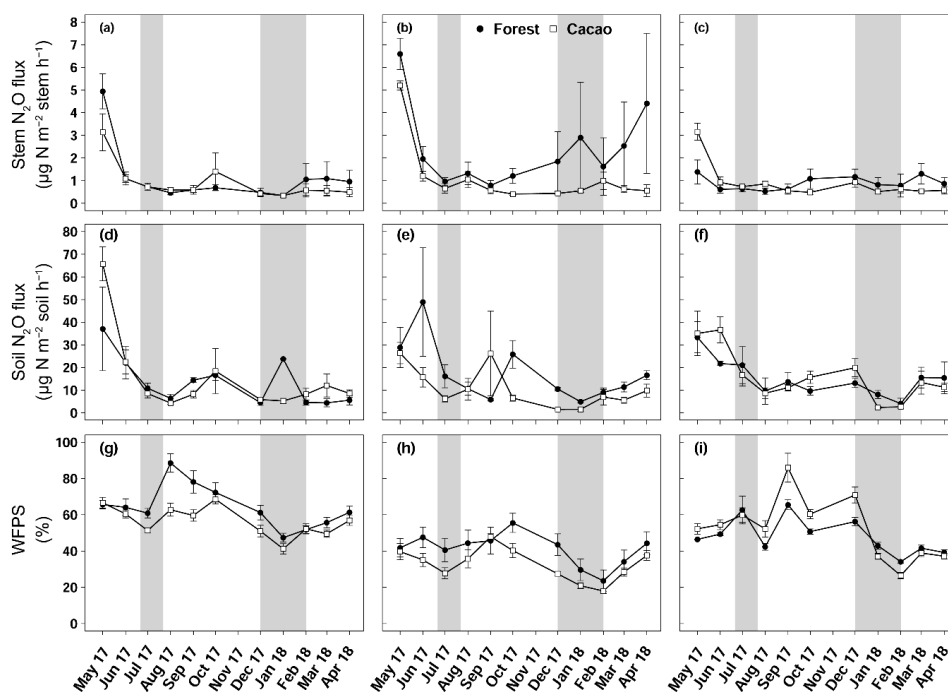
811 ^a Means followed by different lowercase letters indicate significant differences between land-
 812 use types within each site and different capital letters indicate significant differences among the
 813 three sites within a land-use type (linear mixed-effect models with Tukey's HSD at $P \leq 0.05$).



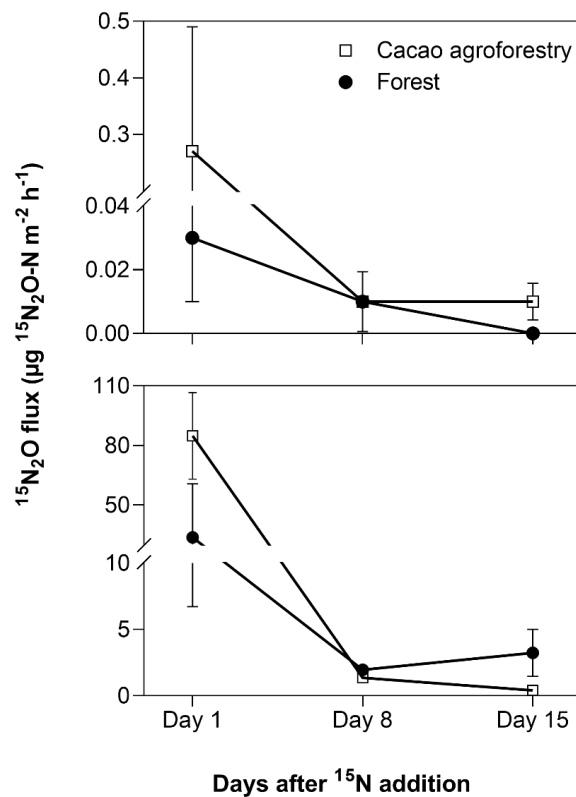
Figures



814 **Figure 1.** Stem N₂O fluxes from 22 tree species at three forest sites (Aloum, Biba Yezoum and
 815 Tomba) across central and south Cameroon in the Congo Basin. Boxes (25th, median and 75th
 816 percentile) and whiskers (1.5 × interquartile range) are based on N₂O fluxes measured monthly
 817 from May 2017 to April 2018 for each tree species, and the values in parentheses represent the
 818 number of trees measured per species. There were no differences in N₂O fluxes among species
 819 (linear mixed-effect models with Tukey's HSD at $P \geq 0.27$).



820 **Figure 2.** Mean (\pm SE, $n = 4$) stem N₂O fluxes (top panel), soil N₂O fluxes (middle panel) and
821 water-filled pore space (bottom panel) in Aloum site (a, d and g), Biba Yezoum site (b, e and
822 h) and Tomba site (c, f and i) in the Congo Basin, Cameroon, measured monthly from May
823 2017 to April 2018; grey shadings mark the dry season.



824 **Figure 3.** Mean (\pm SE, $n = 3$) $^{15}\text{N}_2\text{O}$ fluxes from stems (top panel, unit is per m^2 stem area) and
825 soil (bottom panel, unit is m^{-2} ground area) in the Congo Basin, Cameroon. In May 2018, 290
826 mg ^{15}N (in the form of $(^{15}\text{NH}_4)_2\text{SO}_4$ with 98 % ^{15}N) was dissolved in 8 L distilled water and
827 sprayed within 0.8 m^2 area around each tree (equal to 10 mm rain), which was only 20 % of the
828 extant mineral N in the top 10 cm soil and $49 \pm 1 \%$ and $52 \pm 2 \%$ water-filled pore space for
829 the forest and CAF, respectively, comparable to the soil water content of the site (Fig. 2).



Appendices

830 **Table A1.** Vegetation and site characteristics of the study sites on highly weathered soils in the
 831 Congo Basin, Cameroon. All vegetation characteristics were determined from trees with ≥ 10
 832 cm diameter at breast height in both forest and cacao agroforestry.

Site	Aloum		Biba Yezoum		Tomba	
	Forest	Cacao agroforestry ^a	Forest	Cacao agroforestry ^a	Forest	Cacao agroforestry ^a
Tree density (n ha ⁻¹)	594 ± 29	403 ± 60 (140 ± 37)	619 ± 16	267 ± 24 (96 ± 16)	453 ± 34	430 ± 51 (292 ± 79)
Total basal area (m ² ha ⁻¹)	35 ± 1.4	27 ± 2.5 (1.5 ± 0.5)	33 ± 2.9	27 ± 2.0 (0.9 ± 0.2)	34 ± 2.3	30 ± 3.2 (3.8 ± 1.3)
Legume abundance (% of the number of trees)	7.7 ± 1.7	5.9 ± 1.4	9.3 ± 1.9	6.5 ± 2.3	7.4 ± 1.6	4.8 ± 1.4
Tree height (m)	18.6 ± 0.5	15.1 ± 0.9 (6.8 ± 0.1)	20.6 ± 0.5	16.1 ± 0.4 (6.2 ± 0.3)	19.5 ± 0.4	11.7 ± 1.7 (6.1 ± 0.3)
Diameter at breast height (cm)	23.2 ± 0.6	23.3 ± 1.6 (11.4 ± 0.2)	22.6 ± 0.8	27.2 ± 0.2 (10.8 ± 0.2)	24.8 ± 1.0	23.5 ± 2.7 (12.3 ± 0.6)
Three most abundant tree species in the forest plots at each site ^b	<i>Cleistopholis patens</i> <i>Coelocaryon preussi</i> <i>Pycnanthus angolensis</i>		<i>Celtis sp.</i> <i>Diospyros sp</i> <i>Petersianthus macrocarpus</i>		<i>Celtis sp.</i> <i>Carapa procera</i> <i>Funtumia elastica</i>	
Elevation (m above sea level)		651		674		752
Precipitation ^c (mm yr ⁻¹ ; from 1982 to 2012)		2064		1639		1577

833 ^a For cacao agroforestry, the first values are for both cacao and remnant shade trees, and the
 834 second values in parentheses are for cacao trees only. ^b Determined using Importance Value
 835 Index (IVI = relative density + relative frequency + relative dominance (Curtis and McIntosh,
 836 1951)). For a given species, the relative density refers to its total number of individuals in the
 837 four forest plots at each site; the relative frequency refers to its occurrence among the four forest
 838 plots; and the relative dominance refers to its total basal area in the four forest plots, all
 839 expressed as percentages of all species. ^c Climate-Data.org, 2019.



840 **Table A2.** Seasonal mean (\pm SE, $n = 4$) water-filled pore space (WFPS), extractable mineral N
 841 (measured in the top 5 cm of soil) and nitrous oxide (N₂O) fluxes in forests on highly weathered
 842 soils in the Congo Basin, Cameroon. Means followed by different lowercase letters indicate
 843 significant differences between seasons for each site (linear mixed-effect models with Tukey's
 844 HSD at $P \leq 0.05$).

Season/ site	Stem N ₂ O flux ($\mu\text{g N m}^{-2}$ stem h ⁻¹)	Soil N ₂ O flux ($\mu\text{g N m}^{-2}$ soil h ⁻¹)	WFPS (%)	Soil NH ₄ ⁺ (mg N kg ⁻¹)	Soil NO ₃ ⁻ (mg N kg ⁻¹)
Wet season					
Aloum	1.56 \pm 0.36 ^a	16.7 \pm 3.7 ^a	66.2 \pm 2.2 ^a	6.0 \pm 0.6 ^a	6.0 \pm 0.8 ^a
Biba Yezoum	2.92 \pm 0.73 ^a	22.9 \pm 4.9 ^a	44.8 \pm 2.6 ^a	4.4 \pm 0.3 ^a	2.2 \pm 0.2 ^b
Tomba	1.01 \pm 0.13 ^a	18.6 \pm 2.2 ^a	49.4 \pm 1.8 ^a	6.9 \pm 0.5 ^b	5.4 \pm 0.8 ^a
Dry season					
Aloum	0.61 \pm 0.14 ^b	10.0 \pm 1.8 ^b	62.0 \pm 3.6 ^a	8.7 \pm 1.3 ^a	6.6 \pm 1.0 ^a
Biba Yezoum	1.73 \pm 0.57 ^b	10.3 \pm 1.4 ^b	36.3 \pm 3.2 ^a	5.5 \pm 0.4 ^a	3.6 \pm 0.5 ^a
Tomba	0.69 \pm 0.15 ^b	8.9 \pm 1.9 ^b	46.2 \pm 3.1 ^a	8.7 \pm 0.8 ^a	6.5 \pm 1.1 ^a

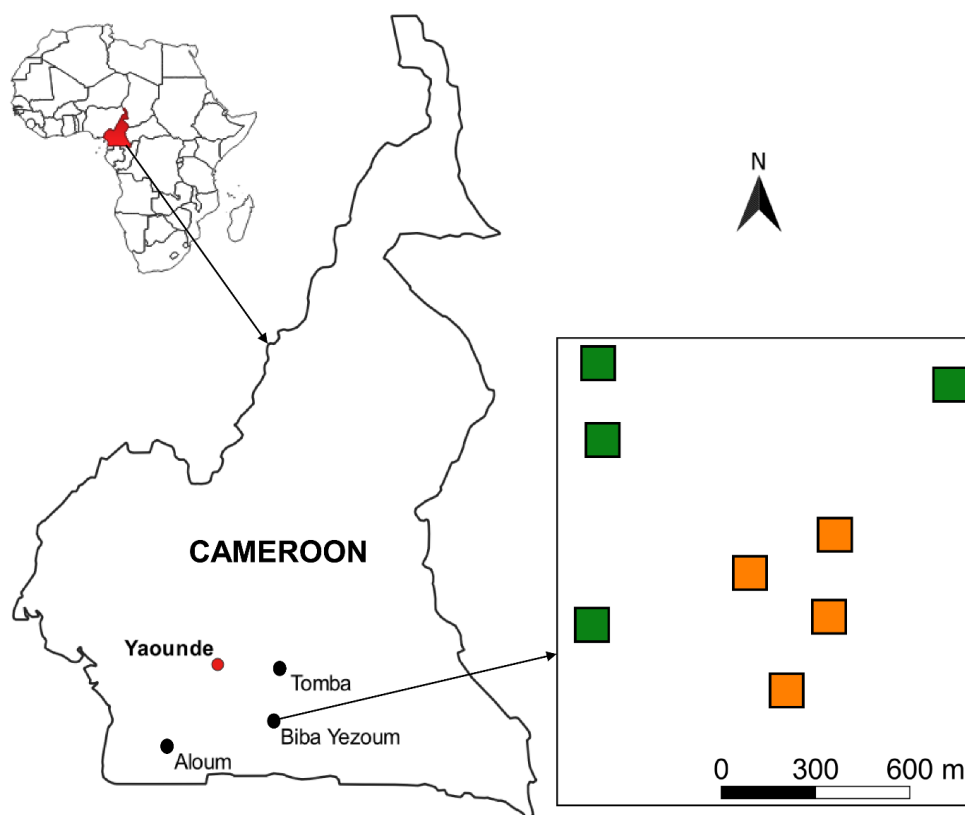


845 **Table A3.** Seasonal mean (\pm SE, $n = 4$) water-filled pore space (WFPS), extractable mineral N
 846 (measured in the top 5 cm of soil) and nitrous oxide (N₂O) fluxes in cacao agroforestry sites
 847 located on highly weathered soils in the Congo Basin, Cameroon. Means followed by different
 848 lowercase letters indicate significant differences between seasons for each site (linear mixed-
 849 effect models with Tukey's HSD at $P \leq 0.05$).

Site/ season	Stem N ₂ O flux ($\mu\text{g N m}^{-2}$ stem h ⁻¹)	Soil N ₂ O flux ($\mu\text{g N m}^{-2}$ soil h ⁻¹)	WFPS (%)	Soil NH ₄ ⁺ (mg N kg ⁻¹)	Soil NO ₃ ⁻ (mg N kg ⁻¹)
Wet season					
Aloum	1.21 \pm 0.27 ^a	22.6 \pm 4.7 ^a	60.3 \pm 1.6 ^a	4.3 \pm 0.4 ^a	2.1 \pm 0.4 ^a
Biba Yezoum	1.43 \pm 0.36 ^a	15.0 \pm 3.5 ^a	38.2 \pm 1.7 ^a	7.0 \pm 0.6 ^a	2.2 \pm 0.4 ^a
Tomba	1.05 \pm 0.18 ^a	21.2 \pm 2.6 ^a	53.4 \pm 2.4 ^a	7.3 \pm 0.8 ^a	2.5 \pm 0.3 ^a
Dry season					
Aloum	0.53 \pm 0.07 ^b	6.4 \pm 0.7 ^b	51.7 \pm 1.9 ^b	6.0 \pm 1.0 ^a	2.7 \pm 0.6 ^a
Biba Yezoum	0.74 \pm 0.12 ^a	5.3 \pm 1.3 ^b	25.9 \pm 1.8 ^b	7.5 \pm 0.6 ^a	3.2 \pm 0.7 ^a
Tomba	0.63 \pm 0.06 ^a	6.2 \pm 1.2 ^b	50.4 \pm 6.2 ^a	6.9 \pm 0.9 ^a	3.4 \pm 0.7 ^a



850 **Appendix B1.** Location of the study sites in Cameroon, showing the four replicate plots per
851 land use (green for forests and orange for cacao agroforestry) at one site.





852 **Appendix B2.** Sampling set-up for stem nitrous oxide (N₂O)-flux measurement at three stem
853 heights in a rainforest in the Congo Basin, Cameroon.





854 **Appendix B3.** Map of the Congo Basin rainforest (green) spanning across the six major Congo
855 Basin countries. Brown shaded area represents the proportion of the Congo rainforest with
856 similar biophysical conditions as our study sites (Ferralsol soils, ≤ 1000 m elevation, and 1500–
857 2100 mm yr⁻¹ precipitation).

